

Does the Singlet Minus Triplet Spectrum with Major Photobleaching Band Near 680–682 nm Represent an Intact Reaction Center of Photosystem II?

Adrien Chauvet,^{†,||} Ryszard Jankowiak,^{*,‡,§} Adam Kell,[‡] Rafael Picorel,[⊥] and Sergei Savikhin^{*,†}

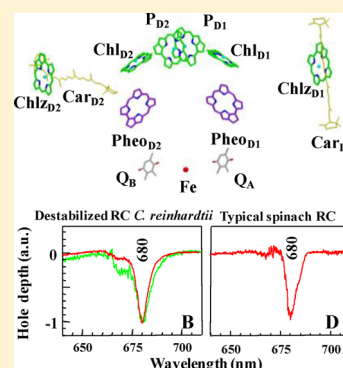
[†]Department of Physics and Astronomy, Purdue University, West Lafayette, Indiana 47907, United States

[‡]Department of Chemistry and [§]Department of Physics, Kansas State University, Manhattan, Kansas 66506, United States

[⊥]Estación Experimental Aula Dei (CSIC), Avda. Montañana 1005, 50059 Zaragoza, Spain

S Supporting Information

ABSTRACT: We use both frequency- and time-domain low-temperature (5–20 K) spectroscopies to further elucidate the shape and spectral position of singlet minus triplet (triplet-bottleneck) spectra in the reaction centers (RCs) of Photosystem II (PSII) isolated from wild-type *Chlamydomonas reinhardtii* and spinach. It is shown that the shape of the nonresonant transient hole-burned spectrum in destabilized RCs from *C. reinhardtii* is very similar to that typically observed for spinach. This suggests that the previously observed difference in transient spectra between RCs from *C. reinhardtii* and spinach is not due to the sample origin but most likely due to a partial destabilization of the D1 and D2 polypeptides. This supports our previous assignments that destabilized RCs (referred to as RC680) (Acharya, K. et al. *J. Phys. Chem. B* **2012**, *116*, 4860–4870), with a major photobleaching band near 680–682 nm and the absence of a photobleaching band near 673 nm, do not represent the intact RC residing within the PSII core complex. Time-resolved absorption difference spectra obtained for partially destabilized RCs of *C. reinhardtii* and for typical spinach RCs support the above conclusions. The absence of clear photobleaching bands near 673 and 684 nm (where the P_{D1} chlorophyll and the active pheophytin (Pheo_{D1}) contribute, respectively) in picosecond transient absorption spectra in both RCs studied in this work indicates that the cation can move from the primary electron donor (Chl_{D1}) to P_{D1} (i.e., P_{D1}Chl_{D1}⁺Pheo_{D1}[−] → P_{D1}⁺Chl_{D1}Pheo_{D1}[−]). Therefore, we suggest that Chl_{D1} is the major electron donor in usually studied destabilized RCs (with a major photobleaching near 680–682 nm), although the P_{D1} path (where P_{D1} serves as the primary electron donor) is likely present in intact RCs, as discussed in Acharya, K. et al. *J. Phys. Chem. B* **2012**, *116*, 4860–4870.



I. INTRODUCTION

Photosystem II (PSII), the only protein complex capable of evolving oxygen, performs primary charge separation (CS) in the D1/D2/Cyt b-559 reaction center (RC)¹ in oxygenic photosynthesis (plants, cyanobacteria, and algae). In this work, we focus on isolated RCs from spinach and *Chlamydomonas reinhardtii*, a unicellular green alga flagellate possessing a single chloroplast. *C. reinhardtii* and spinach are important model systems for fundamental studies of various aspects of photosynthesis. According to a recent X-ray crystal structure² (from *T. vulcanus*), the PSII RC complex contains six chlorophyll (Chl) and two pheophytin (Pheo) molecules, two plastoquinones (Q_A and Q_B), two β -carotene molecules (Car_{D1} and Car_{D2}), Cytochrome b-559 (Cyt b-559), and a nonheme iron. The P_{D1} and P_{D2} Chls are structurally analogous to the P_L and P_M BChls of the bacterial special pair, respectively, while the Chl_{D1,D2} and Pheo_{D1,D2} molecules correspond to the monomeric BChl_{L,M} and BPheo_{L,M} molecules (where the subscripts represent the respective polypeptide chains to which the chlorins are bound).³

Unlike in the bacterial RC (BRC), PSII RCs contain two additional peripheral Chls bound by histidines of the D1 and

D2 polypeptides, and sometimes referred to as Chl_{D1} and Chl_{D2}.⁴ In both BRCs and PSII RCs, the pigments have similar organization and function, with pseudo-C₂ structural symmetry and a functional asymmetry of their two branches D1/L and D2/M.⁵ By analogy with the BRC, it is believed that the D1 protein chain of the PSII RC is photochemically active, and thus the P_{D1}/P_{D2}, Chl_{D1}, and Pheo_{D1} molecules participate in primary CS.¹ The two Chl molecules, P_{D1} and P_{D2}, form a dimer with partial structural overlap, which is stabilized by a van der Waals interaction of about $-17 \text{ kcal mol}^{-1}$.⁶ Differences in the immediate environment of the two pigments of the dimer cause localization of the major portion of the dimer's highest occupied molecular orbital on P_{D1}.⁶ It has also been recently shown that the redox potential (Em) of P_{D1} for one electron oxidation [Em(P_{D1})] is lower than that of P_{D2}, favoring the localization of the cationic charge of the primary charge transfer (CT) state on P_{D1}.⁷

Received: October 4, 2014

Revised: November 25, 2014

Published: December 15, 2014

Many researchers have been interested in electronic structure and ultrafast primary events of oxygenic photosynthesis. Although in recent years consistent progress has been made in comprehending the electronic structure and CT dynamics in isolated PSII RC,^{8–11} an adequate global understanding of this complex system is yet to be achieved. There are still numerous issues regarding primary CS pathways in the PSII RC; for example, the assignment of P_{D1} or Chl_{D1} as primary electron donor is controversial.^{8–12} However, very recently it has been shown by combining two-dimensional electronic spectroscopy and Redfield theory¹³ that, depending on the realization of disorder, both Chl_{D1} and P_{D1} paths are possible in a typical spinach RC. One significant obstacle to the understanding of the PSII RC is that, in contrast to the BRC (which can be isolated and crystallized while maintaining full functionality), the PSII RC is considerably more fragile during isolation and purification procedures^{10,14–16} and retains only limited PSII functionality in its isolated form.^{9,11} Recent spectroscopic studies indeed suggest that the isolated RC from *C. reinhardtii* is more intact than the RC isolated from spinach.^{10,17} In this respect, it has been suggested that the isolated RC samples possess two RC subsets, the destabilized RC680 and the more intact RC684, the latter being vulnerable and changing to RC680 upon biochemical manipulation.^{10,11,17,18} To our knowledge, studies of the isolated intact algal PSII RC from *C. reinhardtii* are only a few, mainly because of the difficulties in preserving its intactness during preparation.^{10,17} It is likely that after isolation, the coupling between P_{D1} , P_{D2} , and other pigments is weakened, resulting in the blue-shift of the Q_y absorption band and modified electron transfer (ET) dynamics.

We argue below that the shapes of transient (nonresonant) holes and time-resolved absorption difference spectra obtained for isolated RCs from *C. reinhardtii* can report on the quality of isolated RC complexes. We use both frequency- and time-domain low-temperature spectroscopies to shed light on the electronic structure and CS, respectively. For simplicity, we focus on the shapes of the 5 K triplet bottleneck holes as well as 20 K transient absorbance changes and decay-associated difference spectra (DADS) measured for both spinach and partly destabilized *C. reinhardtii* isolated RCs. We show that the shape of the transient hole-burned (HB) spectra vary depending on sample quality; for example, after the sample of *C. reinhardtii* is concentrated via centrifugation with a 50 kDa filter to reach a higher optical density (OD) (vide infra), one can observe a transient hole that is typical for spinach RC preparations. High sample concentration is, however, required for time-resolved pump–probe measurements. Therefore, we argue that the previously observed differences in the transient HB spectra for RCs in *C. reinhardtii* and spinach are not due to different sample origins but rather due to the destabilization of the D1 and D2 polypeptides during the sample isolation and concentration procedures.

II. EXPERIMENTAL SECTION

PSII RC complexes from *C. reinhardtii* containing 6 Chls per 2 Pheos were obtained from both thylakoids and PSII-enriched membranes following the method of Nanba and Satoh,¹⁹ with important modifications described in ref 20. Preparation of isolated RCs from both thylakoids and PSII-enriched membranes, as well as basic spectroscopic characterization and pigment analysis, is described in ref 20 (see also Table 1 in the Appendix). The OD at 680 nm was ~ 0.6 in 6 and 0.7 mm cells for HB and pump–probe experiments, respectively. The

sample was concentrated ~ 45 times (from 0.04 up to 1.9 OD in 1 mm) through a centrifuge (by a series of 5 min cycles at $\sim 6000g$ in a tabletop centrifuge at 4 °C). Besides glycerol, no other chemicals were added. Spinach PSII RCs were isolated as described in ref 14.

The hole burning apparatus and measurements were described in detail elsewhere.²¹ Briefly, a Bruker HR125 Fourier transform spectrometer and a Janis 8-DT Super Vari-Temp liquid helium cryostat were used to measure the absorption and HB spectra at 5 K. Nonresonant HB spectra were recorded at a resolution of 4 cm^{-1} using a burn wavelength (λ_B) of 496.5 nm from a Coherent Innova 200 argon ion laser or 665.0 nm from a tunable Coherent CR699–21 ring dye laser (Exciton LD688; line width of 0.07 cm^{-1}) pumped by a 532 nm Spectra-Physics Millennia 10 s diode laser. The laser output was stabilized using LPC from Brockton Electro-Optics Corp. Sample temperature was read and stabilized with a Lakeshore Cryotronic model 330 temperature controller. The transient spectra reported in this work corresponded to the difference between the absorption spectrum with laser on and the absorption spectrum with laser off. This difference is due to dynamic depopulation of the singlet ground state for the duration of the (long) lifetime of either the triplet state (triplet-bottleneck hole) or CS state. Burn intensities and times are given in the figure captions.

The optical pump–probe spectroscopy system has been described in detail elsewhere.²² The 780 nm, ~ 100 fs long pulses from a self-mode-locked Ti:sapphire laser were amplified by a factor of $\sim 10^5$ at 1 kHz repetition rate in a regenerative amplifier and converted to infrared signal and idler pulses in a type I BBO optical parametric amplifier. The signal output pulses were frequency-doubled into tunable visible light pulses (600–730 nm), which served as sample excitation (pump) pulses. The transient absorption of a sample upon excitation was probed with broadband femtosecond continuum light pulses generated in a sapphire plate using a fraction of the amplifier output; cross correlations between the pump and probe pulses were typically 100–200 fs fwhm. A fraction of the continuum beam was used as a reference. After passing through the sample, both probe and reference beams were dispersed in an Oriel MS257 imaging monochromator operated at a 2.5 nm bandpass and directed onto separate Hamamatsu S3071 Si pin photodiodes. The pump beam intensity was monitored and digitized, along with the transmitted signal and reference beams, hence permitting real-time noise monitoring. The sample was housed in a closed cycle liquid helium-cooled cryostat (Air Products DE202, Allentown, PA) and all transient experiments were performed at 20 K.

III. RESULTS AND DISCUSSION

3.1. Absorption Spectra of Isolated PSII RCs from *C. reinhardtii*. Figure 1 (top frame) shows the Q_y -region absorption spectra (a–d) of various isolated PSII RC samples from *C. reinhardtii*. The spectra (a–d) were obtained for RC preparations referred to below as samples A, B, C, and D, respectively. We showed recently that a typical RC from *C. reinhardtii* is represented by spectrum (a) (black curve, sample A), while the most intact RCs are represented by curve (d) (red curve, sample D).¹⁰ The latter is very difficult to obtain even in very small quantities, and its spectrum is replotted here for comparison from ref 10, in which this sample was studied in great detail by hole-burning spectroscopy.

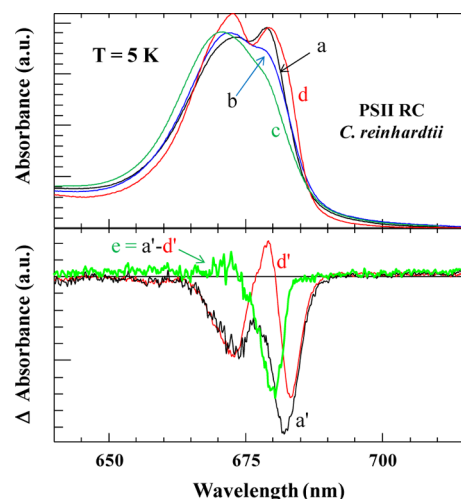


Figure 1. Top frame: (a–d) represent 5 K absorption spectra obtained for isolated RC from *C. reinhardtii* at different level of intactness. Curves (a–d) are normalized for the same integrated intensity in the Q_y -region. Bottom frame: Curves (a') (black) and (d') (red) are nonresonant transient holes ($\lambda_B = 665.0$ nm) measured for the samples with absorption spectra (a) and (d), respectively. Spectrum (e) is the difference between curves (a') and (d') (see text).

Spectral changes in the Q_y -region are similar to those observed in our laboratories for spinach RC over the years. Spectrum (a) is similar to absorption spectra of the widely studied spinach RC (see also Figure 3C). Spectrum (b) was obtained for sample A after a concentration procedure to increase its OD; the higher OD sample (below referred to as sample B) was required in order to increase the signal-to-noise ratio for time-resolved pump–probe measurements reported below. All pump–probe experiments for *C. reinhardtii* (vide infra) were obtained for sample B, which due to the concentration procedure is in part destabilized as reflected by different shapes of spectra a and b in Figure 1. Interestingly, HB studies repeated on sample B about two months later (after pump–probe measurements) revealed further destabilization (see absorption spectrum (c) in Figure 1 and corresponding transient hole (b) shown in Figure 2A). The latter sample is referred to below as sample C. Thus, curves (a–c) represent samples with a different degree of destabilization compared to sample D [represented by curve (d)].

As indicated by the changes in absorption spectra (a–d), it is obvious that the RC samples from *C. reinhardtii* are not very stable. A partial structural destabilization can easily occur in isolated RC proteins, leading to somewhat different absorption spectra. Curve (b) in Figure 1 has a similar shape to that of partially damaged spinach RCs (data not shown), while spectrum (a) of Figure 1 (for *C. reinhardtii*) is very similar to the absorption spectrum of typical spinach RCs (see Figure 3C). Curve (c) (sample C) in Figure 1 and the corresponding transient hole with additional bleach near 669 nm [curve (b) in Figure 2A] is similar to the previously studied strongly destabilized spinach RC,²³ for which an additional transient hole near 669 nm was observed (not shown). Interestingly, although such samples were strongly destabilized, resonant burning in the 680–682 nm region yielded a fast decay time for P680* of 1.9 ± 0.2 ps at 4.2 K.

We believe that the broadening and blue-shift of the absorption spectra shown in Figure 1 (that over the years was also reported for spinach RCs; for example, see refs 10, 11,

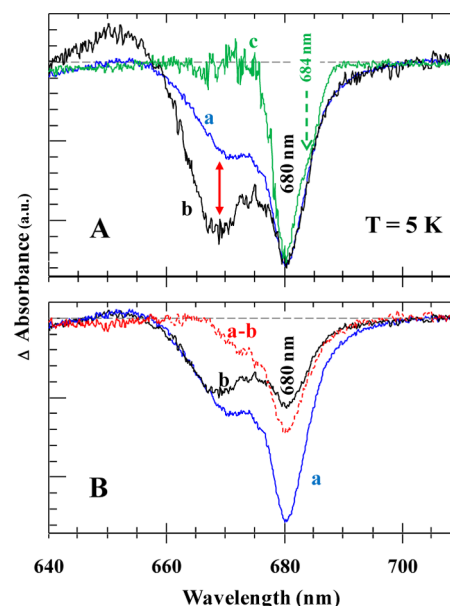


Figure 2. Spectra (a) and (b) in panels A and B correspond to differently normalized transient holes obtained for isolated RCs from *C. reinhardtii* (i.e., for the strongly destabilized sample C) using $\lambda_B = 496.5$ and 665.0 nm, respectively. Both curves (a) and (b) in frames A and B were normalized near 680 and 665 nm, respectively. (A) Spectrum (c) is a typical transient hole obtained for spinach RC using $\lambda_B = 665.0$ nm; the weak shoulder near 683–684 nm was previously assigned to the RC684.¹⁰ (B) The red curve is the difference between spectra (a) and (b), which were normalized near 665 nm.

15–17, and 23) is due to modification of the pigment–protein interactions that may affect the electronic structure of RCs²⁴ and/or Chl ring deformation.²⁵ For example, the Q_y -absorption band of Pheos also shifts to higher energies [i.e., the band maxima corresponding to spectra (d), (a), (b), and (c) are 544.0, 543.0, 543.0, and 541.8 nm, respectively] (spectra not shown for brevity; see also refs 15, 16, and 23). However, we emphasize that such behavior has nothing to do with the extraction of pigments since absorption spectra similar to (b) and (c) were previously obtained for spinach RC without and with TX-100 detergent.¹⁶ Therefore, these data confirm that the changes observed in absorption spectra are due to perturbations of the pigment–protein structure.

3.2. Transient HB Spectra of Isolated PSII RCs from *C. reinhardtii* and Spinach. Transient holes discussed below are due to dynamic depopulation of the singlet ground state for the duration of the (long) lifetime of either the triplet state (triplet-bottleneck hole, in the absence of Q_A) and/or CS state ($P_{D1}^+Q_A^-$ in systems where Q_A is present).¹⁰ We have recently proposed that spectrum (d) and the corresponding transient hole (d') in Figure 1 (lower frame) represent the most intact RC studied so far for isolated RCs from *C. reinhardtii*, with the major photobleaching bands near 684 and 673 nm. We have also demonstrated that a large fraction of RCs in sample D also contained Q_A ,¹⁰ while in most isolated RC samples studied so far Q_A was lost during the preparation/purification procedures. These isolated RCs showed transient holes near 680–684 nm and no photobleaching band near 673 nm, where the special pair pigments (P_{D1}/P_{D2}) contribute;⁸ indicating that the triplet state is not localized on the special pair pigments (i.e., P_{D1} or P_{D2} Chls). A typical transient HB spectrum obtained for *C. reinhardtii* (sample A) is shown in Figure 1B [curve (a'), black].

We hasten to emphasize that typical transient (triplet-bottleneck) holes observed in all spinach RCs are characterized by a single bleaching band near 680 nm, with a weak shoulder near 683–684 nm^{10,26–28} (see also Figure 3D). However, strongly destabilized RCs also have a broad bleaching band near 669 nm, as shown in Figure 2. We recently argued¹⁰ that the RC absorption spectrum from *C. reinhardtii* [similar to curve (a) in Figure 1] contains contributions from a mixture of at least two RC subpopulations referred to as RC680 and RC684 in the literature.^{10,17} Previously, the 680 nm contribution (assigned to RC680) was obtained by subtracting spectra measured for the same RC preparation but with different burning wavelength¹⁰ [i.e., $\lambda_B = 665.0$ and 496.5 nm]. Here we use the same burning wavelength ($\lambda_B = 665.0$ nm) and compare data obtained for samples A and D, with sample A being partly destabilized (less intact sample) and sample D corresponding to the most intact sample obtained so far. The result is the same as shown in Figure 1 (lower frame) by the green curve (e) = (a') – (d'), which also reveals an additional (transient) bleaching band near 680 nm as typically observed for isolated spinach RCs (i.e., RC680).^{26,27} That is, curve (e) was obtained by subtracting the contribution of intact RCs [curve (d')] from the spectrum of partially destabilized RCs [curve (a')] after mutual normalization at the low-energy side of the HB spectra. As expected, the extracted spectrum has a major photo-bleaching band near 680 nm with no contribution near 683–684 and 673 nm [curve (e)]. In fact, this band is very similar to that often reported for isolated spinach RC;^{26,27} compare with the transient hole for spinach RC in Figure 3D. As before, we assign these transient holes to be representative of a RC680 (less intact) subpopulation of RCs.

We now turn to the transient holes obtained for sample C of *C. reinhardtii*. Spectra (a) and (b) in both frames of Figure 2 show (nonresonant) transient holes obtained using $\lambda_B = 496.5$ and 665.0 nm, respectively. In Figure 2A, curves (a) and (b), are mutually normalized near 685 nm, while in frame B the same curves (a) and (b) are normalized at 665 nm to demonstrate that the bands near 669 (red arrow) and 680 nm are caused by different subpopulations of RCs. Recall that the 669 nm band is only observed in strongly destabilized/damaged samples. This is consistent with the 669 nm band not being observed for an excitation wavelength near 680–684 nm (data not shown). Spectrum (c) in Figure 2A is a transient hole obtained for the best spinach RC studied in our laboratory over the years using the same $\lambda_B = 665.0$ nm. As expected, this spinach RC sample (with a major bleach near 680 nm) does not reveal any bleach near 669 nm, but there is also no bleach near 684/673 nm as observed in the most intact RCs from *C. reinhardtii* (see curve (d') in Figure 1, which closely resembles the RCs within the PSII cores^{8,18,29,30}), suggesting that the D1/D2/Cyt b-559 sample from spinach is partly destabilized. The very weak shoulder near 683–684 nm in curve (c) in Figure 2A (dashed green arrow) was also previously observed^{26,27} and is assigned to a small contribution from the RC684 (lacking Q_A) with Chl_{D1} serving as the primary electron donor^{10,11} (i.e., with the triplet state localized on Chl_{D1}). A comparison of spectra (a) and (b) (for *C. reinhardtii*) with spectrum (c) (for spinach) near 680–684 nm in Figure 2A reveals that strongly destabilized *C. reinhardtii* (sample C) has significantly more contribution from the 669 nm band and relatively higher subpopulation of more intact RC684 (i.e., the 680 nm band is slightly broader due to the additional contribution from RC684; vide infra). The difference (a) – (b) between the

normalized spectra (a) and (b) in Figure 2B is dominated by the 680 nm band, clearly indicating that the latter bleach originates from destabilized RCs.

To further demonstrate that the bleach near 680 nm does not represent an intact PSII RC, Figure 3 shows absorption and

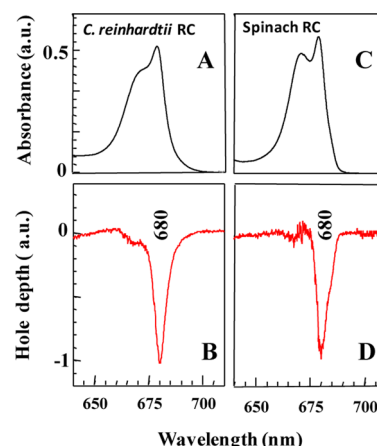


Figure 3. (A and B) Absorption and transient HB spectra obtained for destabilized *C. reinhardtii* and (C and D) a typical spinach RC. $T = 5$ K. HB spectra were obtained with $\lambda_B = 665.0$ nm and laser intensity of $\sim 100 \text{ mW cm}^{-2}$.

transient holes for destabilized *C. reinhardtii* (panels A and B, respectively) and one of the best spinach RC samples studied in our laboratory (panels C and D, respectively). Note that the resulting transient holes in Figure 3 (panels B and D) are very similar.

Given the above results (and data published recently; see refs 10 and 17), we conclude that typical RCs isolated from *C. reinhardtii* studied by our groups can be easily destabilized during the concentration or dilution procedures. Since larger destabilization leads to a larger contribution from RC680 (associated with the bleaching band near 680 nm), we suggest that spinach RC, with a major bleaching band near 680 nm, is not representative of the intact RCs. Consequently, such spectra should not be used to adequately model the intact RCs residing inside the PSII core complex.

3.3. Time-Resolved Absorption Difference and DADS.

We begin with the data obtained for spinach RCs shown in Figure 4. Panels A and B show transient absorption difference

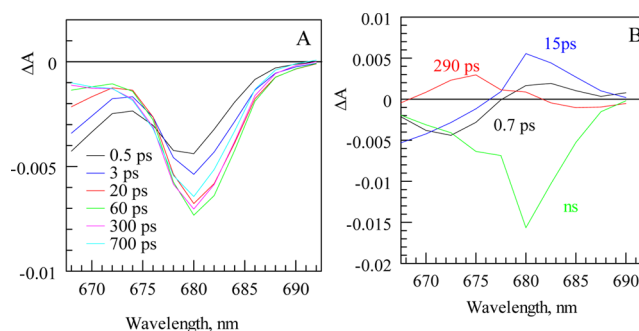


Figure 4. (A) Broad ΔA spectra measured for spinach RC at 20 K for different delay times (from 0.5–700 ps) after excitation ($\lambda_{\text{ex}} = 665$ nm). (B) DADS obtained for ΔA kinetics recorded from –20 to 700 ps for a series of probe wavelengths taken at every 2.5 nm for spinach RC.

spectra (ΔA) and DADS, respectively. All time-dependent absorption difference profiles were recorded at $T = 20$ K for a time range from -20 to 700 ps using 665.0 nm excitation pulses. Upon excitation, the major transient absorption bleaching band in spinach RC emerges near 680 nm (Figure 3A), in agreement with other studies.^{13,31,32} A minimum of four decay components was necessary to globally fit the kinetics probed between 665.0 – 700.0 nm with a step size of 2.5 nm. The respective amplitudes of each component are shown in Figure 4B as a function of probe wavelength (DADS). Selected kinetics that served to produce the DADS spectra and their fits are shown in the Supporting Information.

The spectra of 0.7 and 15 ps decay components (Figure 4B) reveal a bimodal signal with a positive maxima around 680 – 683 nm. Such bimodal feature is typical of energy transfer, and consequently, both components are assigned to a rapid energy transfer from higher energy pigments excited by the pump pulse to the state that absorbs at 680 – 683 nm. This resulting state is associated with the longer ns-DADS component, as the latter component is maximized at 680 nm. Note that since our temporal window extended only to 700 ps, precise evaluation of the nanosecond component lifetime was not possible. Thus, we will keep referring to it as a nanosecond (ns)-long component in the rest of the manuscript. The 680 nm bleaching feature of the ns DADS component is consistent with the absorption band of the active Pheo_{D1}. This assignment is consistent with previously reported experiments involving dithionite plus white light reduction of Pheo to Pheo[−], where it was shown that the Pheo Q_y state (active in CS) in isolated spinach RCs lies near 680 nm.¹⁵ The 673 – 675 nm shoulder in the ns-DADS component could be assigned to oxidized P_{D1} (or P_{D2}). Consequently, we suggest that the excitation leads to an initial reduction of Pheo_{D1} with lifetimes of 0.7 and 15 ps, followed by a slow \sim nanoseconds recombination. Similar ns-long recombination timescales were observed before in isolated PSII RC from spinach.³¹ Thus, it is likely that P_{D1} could serve as the primary electron donor (see below), though one cannot entirely exclude that the cation on Chl_{D1} (i.e., Chl_{D1}⁺) could move to P_{D1} (i.e., P_{D1}⁺) in the following CT sequence: P_{D1}Chl_{D1}⁺Pheo_{D1}[−] \rightarrow P_{D1}⁺Chl_{D1}Pheo_{D1}[−].

The 290 ps DADS component (Figure 4B) shows a negative band at ~ 685 nm (i.e., photobleaching decay) that is mirrored by the positive band at 673 – 675 nm (i.e., photobleaching rise). This component is assigned to excitation energy transfer (EET) from the red-most pigments, absorbing above 682 nm, toward the special pair P_{D1}/P_{D2}, which absorbs near 673 – 675 nm when the special pair is in the ground state. Such a slow uphill EET is expected at low temperatures. It is possible that a fraction of red pigments are either directly excited by a pump pulse at 665 nm via their blue vibronic band(s) or are populated via rapid downhill EET.

Figure 5 shows ΔA spectra (frame A) and DADS (frame B) obtained for *C. reinhardtii* RC (sample B). These spectra were also obtained using $\lambda_{\text{ex}} = 665.0$ nm at 20 K. Similar to the data from spinach RC (Figure 4B), this data set can also be globally fitted with a minimum of four decay components (vide supra). The resulting DADS in Figures 4B and 5B are comparable, which clearly indicates that the energy and ET processes are similar in both RCs. However, the ΔA spectra in Figure 5A, as well as the 0.8 and 15 ps DADS components (Figure 5B), maximize at ~ 2 nm longer wavelength, when compared to the corresponding spectra from spinach. Also, the long ns-DADS component is broader for *C. reinhardtii* and also red-shifted in

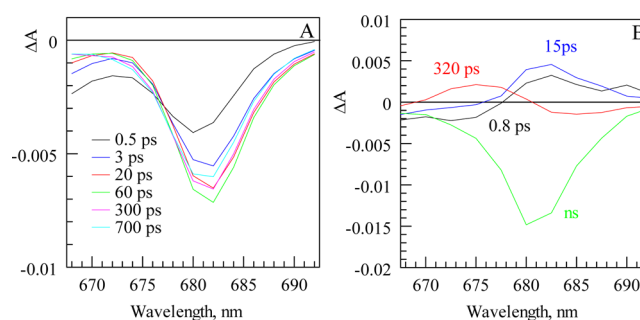


Figure 5. (A) Broad ΔA spectra obtained for *C. reinhardtii* RC at 20 K for different delay times (0.5 – 700 ps) after excitation ($\lambda_{\text{ex}} = 665$ nm). (B) DADS based on kinetics (-20 to 700 ps) probed at every 2.5 nm for *C. reinhardtii*.

respect to the ns-DADS component for spinach RCs (compare ns-DADS profiles in Figures 5B and 4B, respectively). While these shifts are not substantial, they are reproducible and agree with the general trend revealed in static spectra (Figures 1–3) for preparations containing different ratios of less- (RC680) and more-intact (RC684) complexes.

Thus, we infer that the data shown in Figure 5B supports the conclusion that *C. reinhardtii* samples contain a relatively higher fraction of intact RC684 than spinach samples. To highlight the differences between the species, Figure 6 shows differences between ΔA spectra taken at different time delays for both RC samples (*C. reinhardtii* and spinach) (i.e., $\Delta\Delta A = \Delta A_{\text{reinhardtii}} - \Delta A_{\text{spinach}}$).

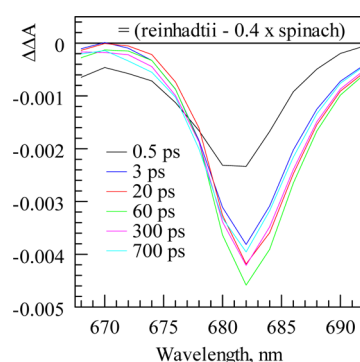


Figure 6. Differences between the ΔA spectra of *C. reinhardtii* and spinach ($\times 0.4$) at different delay times. The factor of 0.4 is the correction that was systematically applied to the ΔA spectra from spinach RC in order to normalize the 670 nm region of spinach with that of *C. reinhardtii*.

Indeed, the double-difference spectra shown in Figure 6 reveal the presence of a subpopulation in *C. reinhardtii* whose band maximizes above 680 nm. The fitting of these $\Delta\Delta A$ signals in the 680 to 690 nm region requires a minimum of two rising times of 0.5 and 18 ps followed by a nanosecond-long decay time, similar to the DADS components observed for spinach RCs. We therefore infer that this subpopulation represents a CS state (i.e., Chl_{D1}⁺Pheo_{D1}[−]) and is consequently ascribed to the more intact RCs.

The transient data therefore agrees with the presence of two different types of RCs in the *C. reinhardtii* sample: one whose major transient photobleaching band maximizes at 680 nm and the other that maximizes at 682 – 684 nm. The latter band is

assigned to the intact RCs, while the former is ascribed to partially destabilized RC complexes.

In these experiments, the expected 673 nm shoulder, which is indicative of P_{D1} or P_{D2} participation in the CS state, is not clearly resolved due to its proximity to the pump wavelength (665 nm). In order to avoid such interferences, the RCs were also excited at 690 nm, and the respective ΔA profiles are shown in Figure 7 for spinach and in Figure 8 for *C. reinhardtii*.

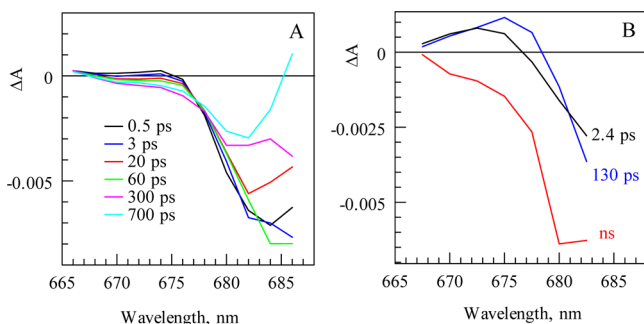


Figure 7. (A) ΔA spectra for spinach RC taken at different time delays as a function of probe wavelength after exciting it at 690 nm. (B) DADS based on ΔA kinetics (-20 to 700 ps) probed at every 2.5 nm for spinach.

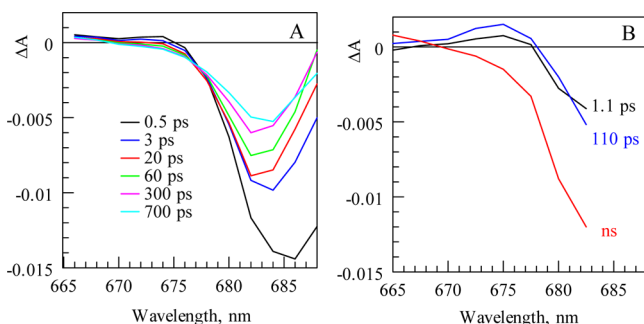


Figure 8. (A) ΔA spectra for *C. reinhardtii* taken at different time delays after excitation at 690 nm. (B) DADS based on ΔA kinetics (-20 to 700 ps) probed at every 2.5 nm for *C. reinhardtii*.

The 690 nm excitation (Figure 7A) of spinach RC reveals the ~ 673 nm shoulder that corresponds to the ΔA signal reported by ref 31 and ascribed to P_{D1}^+ as part of the final radical pair state. Three decay components are required to fit the corresponding set of kinetics, and the generated DADS are shown in Figure 7B. The 2.4 and 130 ps components can be ascribed to EET or ET from the initially excited species absorbing at ~ 690 nm to the pigments absorbing at ~ 672 and ~ 675 nm, respectively. The 672–675 nm pigments most likely represent the special pair Chls. The longer 130 ps component is consistent with a slow uphill EET, as expected at low temperature. However, the 2.4 ps dynamics are too fast for uphill transfer at 20 K and must be primarily due to the formation of a radical state involving the $P_{D1/D2}$ pigments. The long ns-DADS component is representative of the final radical pair state, maximizing near 680 nm with a shoulder in the 670 nm region, similar to that reported by ref 31.

Figure 8 shows the analogous data for *C. reinhardtii* obtained with 690 nm excitation. It is interesting to note that although the ΔA spectra taken at different time delays for *C. reinhardtii* (Figure 8A) look similar to those obtained for spinach RC (Figure 7A), the 670 nm shoulder in *C. reinhardtii* is

qualitatively about twice smaller in amplitude, though a more precise quantitative analysis is not possible due to its small amplitude and overlap with the strong photobleaching band at 680–685 nm. The photobleaching band in the ΔA spectrum of *C. reinhardtii* also differs from that of spinach, as it maximizes at longer wavelength. However, the decay times and shape of the DADS components for both species (Figures 7B and 8B) are comparable, though the long ns-component lacks the shoulder at around 670 nm in the case of *C. reinhardtii* and maximizes at a longer wavelength, as shown in Figure 8B. Again, we ascribe the pigment pool that absorbs near 684 nm to the more intact RCs that are more abundant in *C. reinhardtii*, though as mentioned above, sample B was already partially destabilized. The fact that Figure 6 shows signals (i.e., $\Delta\Delta A$) maximizing near 682 nm, while Figure 8 shows signal maximizing near 683–684 nm, is most probably a result of the pump wavelength being different; that is, under 690 nm excitation, the intact RCs are preferentially excited, while the 665 nm laser pump excites both the destabilized (RC680) and the more intact RC684 RCs. The ΔA signal at wavelength above 680 nm is ascribed to the expected bleaching of P_{D1} from intact RCs in *C. reinhardtii*, which is also expected to be slightly red-shifted. The smaller signal contributing in the 670–675 nm region for *C. reinhardtii* (Figure 8A), compared to the corresponding data obtained for spinach RC (Figure 7A), indicates a weaker contribution to the signal from the $P_{D1/D2}$ pigments. This suggests that $P_{D1/D2}$ pigments are probably not involved in the final radical pair state in intact RCs from *C. reinhardtii*. Thus, it cannot be excluded that the weak signal near 670 nm in spinach RCs originates from a small fraction of photodamaged RCs associated with the transient hole observed near 670 nm in damaged RC from *C. reinhardtii* (see Figure 2). Such holes were also observed in partly damaged spinach RCs (data not shown).

In order to reveal a larger contribution from intact RCs in *C. reinhardtii*, in Figure 9 we reanalyze the kinetic data measured

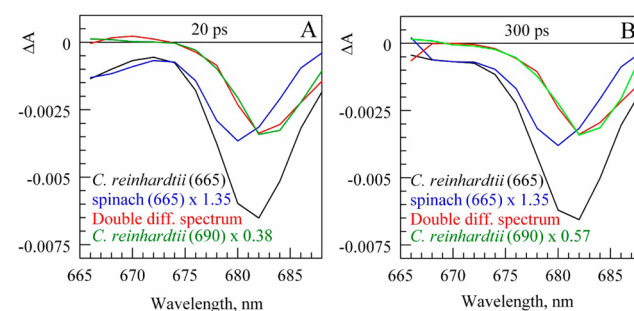


Figure 9. Difference (red) between the ΔA spectra measured at (A) 20 and (B) 300 ps for RC complexes from *C. reinhardtii* (black) and spinach (blue) for excitation wavelength of 665.0 nm. The ΔA spectra for spinach have been normalized in amplitude so that the difference spectrum (red) best fits the normalized spectra shape of *C. reinhardtii* (see text for details), while exciting it at 690.0 nm (green).

at 20 and 300 ps after 665.0 nm laser excitation. We start by normalizing the ΔA signals for spinach and *C. reinhardtii* near 670 nm (see the blue and black curves, respectively). The normalization factor of 1.35 accounts for the differences in excitation pulse intensity used for spinach and *C. reinhardtii* RCs. The signal difference (Figure 9, red curves) reveals in both frames a band near 684 nm, whose shape is nearly indistinguishable from the ΔA spectra obtained for the *C.*

Table 1. Isolation and Purification of Photosystem II Reaction Centers

organism	spinach (<i>S. oleracea</i>)	<i>C. reinhardtii</i>
detergent	Triton X-100, β -DM	Triton X-100, β -DM
isolation conditions	extraction with Triton X-100 from PSII-enriched membranes, differential centrifugation at 100000g, DEAE ionic-exchange chromatography, washing column with 30 mM NaCl, Triton X-100 exchange with β -DM, NaCl gradient	extraction with Triton X-100 from thylakoid membranes, differential centrifugation at 150000g, DEAE ionic-exchange chromatography, washing column with 200 mM NaCl, Triton X-100 exchange with β -DM, NaCl gradient
Chl/P680	6	6
Pheo/P680	2	2
Q _A /P680	lost	partly present
Q _B /P680	lost	lost
Mn cluster	destroyed	destroyed
subunit composition	D1, D2, Cyt b-559	D1, D2, Cyt b-559

reinhardtii RCs using 690.0 nm laser excitation (green curves). Recall that the 690.0 nm excitation pulses preferentially excite intact RCs. We assign the 684 nm band to a contribution from the intact RCs (i.e., RC684). To align the red and green curves, the latter curves in frames A and B were multiplied by factors 0.38 and 0.57, respectively. We conclude that this data supports our earlier conclusion that the isolated RCs from *C. reinhardtii* possess a larger fraction of the intact RCs (i.e., RC684). A similar conclusion was reached analyzing the ΔA spectra recorded at 3 and 60 ps (not shown).

IV. CONCLUDING REMARKS

The data from both HB and TA experiments suggests that RCs isolated from *C. reinhardtii* contain a higher fraction of intact RCs (i.e., RC684) than isolated spinach RCs. The subpopulation of intact RCs is characterized by a photobleaching band maximizing at ~ 684 nm, instead of the 680 nm band that is ascribed to partially destabilized RCs. The latter is in agreement with the data obtained for PSII core complexes in which RCs have red-shifted absorption spectra.³³ The low signal in the 673 nm region in *C. reinhardtii* RCs measured after 690 nm excitation (which mostly excites the intact RCs), suggests that P_{D1} is not involved in the final radical pair state in RCs studied in this work. However, both RCs studied in this work were partly destabilized. This needs to be confirmed by further transient studies in the 545 and 450 nm region where the Pheo Q_x and Pheo anion photobleaching is monitored in both intact spinach and intact *C. reinhardtii* RCs, assuming that intact RCs can be obtained at high OD necessary for time-domain experiments. Until this issue is resolved, we tentatively suggest that isolation of PSII RCs leads to destabilized D1 and D2 proteins, leading to the dominant Chl_{D1} pathway for CS in isolated PSII RCs. That is, the nature of the primary electron donor in isolated RCs most likely depends on the intactness of the protein. On the basis of these results, we question the validity of using optical spectra obtained from isolated spinach RCs to model the intact PSII core complexes.³⁴ The pigment site energies extracted by modeling isolated RCs from spinach may not be valid to properly model the native intact RC residing inside the PSII core complex, and as a result, their values may need to be revised. We suggest that (at least for the RC samples studied in this work) Chl_{D1} is the major electron donor in both spinach and *C. reinhardtii*; although it cannot be excluded that more intact samples (in particular the ones where Q_A is present) could reveal the presence of two ET pathways, where both Chl_{D1} and P_{D1/D2} could serve as primary electron donors. Only then, various CT states (i.e., P_{D1}⁺P_{D2}⁻, P_{D2}⁺P_{D1}⁻, P_{D2}⁺Pheo_{D1}⁻, and P_{D1}⁺Pheo_{D1}⁻) should be taken into account

in a theoretical description of various linear and nonlinear spectra obtained for isolated spinach RCs.

■ APPENDIX

Table 1 provides information regarding isolation and purification of Photosystem II Reaction Centers.

■ ASSOCIATED CONTENT

Supporting Information

Selected kinetics that served to produce the DADS spectra and their fits. This material is available free of charge via the Internet at <http://pubs.acs.org>.

■ AUTHOR INFORMATION

Corresponding Authors

*E-mail: ryszard@ksu.edu.

*E-mail: sergei@purdue.edu.

Present Address

^{||}Ecole Polytechnique Fédérale de Lausanne (EPFL), Laboratoire de Spectroscopie Ultrarapide, ISIC, Faculté des Sciences de Base, Station 6, 1015 Lausanne, Switzerland.

Notes

The authors declare no competing financial interest.

■ ACKNOWLEDGMENTS

The authors acknowledge the Division of Chemical Sciences, Geosciences, and Biosciences, Office of Basic Energy Sciences of the U.S. Department of Energy through Grant DE-FG02-09ER16084 (to S.S.) and DE-FG02-11ER16281/DE-SC0006678 (to R.J.) for support. Samples were prepared by R.P. at the National Renewable Energy Laboratory (NREL), Golden CO (in Dr. Michael Seibert's laboratory) during his leave from the Estación Experimental Aula Dei (CSIC). The latter work was supported by the MINECO (Grant AGL2011-23574). We also thank Dr. K. Acharya for help at the early stage of this project and Dr. M. Seibert (NREL) for useful discussions.

■ REFERENCES

- (1) Diner, B. A.; Rappaport, F. Structure, Dynamics, and Energetics of the Primary Photochemistry of Photosystem II of Oxygenic Photosynthesis. *Annu. Rev. Plant Biol.* **2002**, *53*, 551–580.
- (2) Umena, Y.; Kawakami, K.; Shen, J.-R.; Kamiya, N. Crystal Structure of Oxygen-Evolving Photosystem II at a Resolution of 1.9 Å. *Nature* **2011**, *473*, 55–60.
- (3) Deisenhofer, J.; Epp, O.; Miki, K.; Huber, R.; Michel, H. X-Ray Structure Analysis of a Membrane Protein Complex: Electron Density Map at 3 Å Resolution and a Model of the Chromophores of the

Photosynthetic Reaction Center from *Rhodospseudomonas viridis*. *J. Mol. Biol.* **1984**, *180*, 385–398.

(4) Xiong, J.; Subramanian, S.; Govindjee. A Knowledge-Based Three Dimensional Model of the Photosystem II Reaction Center of *Chlamydomonas reinhardtii*. *Photosynth. Res.* **1998**, *56*, 229–254.

(5) Trebst, A. The Topology of the Plastoquinone and Herbicide Binding Peptides of Photosystem II in the Thylakoid Membrane. *Z. Naturforsch.* **1986**, *41c*, 240–245.

(6) Nilsson Lill, S. O. On the Dimerization of Chlorophyll in Photosystem II. *Phys. Chem. Chem. Phys.* **2011**, *13*, 16022–16027.

(7) Saito, K.; Ishida, T.; Sugiura, M.; Kawakami, K.; Umena, Y.; Kamiya, N.; Shen, J.-R.; Ishikita, H. Distribution of the Cationic State over the Chlorophyll Pair of the Photosystem II Reaction Center. *J. Am. Chem. Soc.* **2011**, *133*, 14379–14388.

(8) Renger, T.; Schlodder, E. Primary Photophysical Processes in Photosystem II: Bridging the Gap between Crystal Structure and Optical Spectra. *ChemPhysChem* **2010**, *11*, 1141–1153.

(9) Cox, N.; Hughes, J.; Rutherford, A. W.; Krausz, E. On the Assignment of PSHB in D1/D2/cytb₅₅₉ Reaction Centers. *Phys. Procedia* **2010**, *3*, 1601–1605.

(10) Acharya, K.; Zazubovich, V.; Reppert, M.; Jankowiak, R. Primary Electron Donor(s) in Isolated Reaction Center of Photosystem II from *Chlamydomonas reinhardtii*. *J. Phys. Chem. B* **2012**, *116*, 4860–4870.

(11) Jankowiak, R. Probing Electron-Transfer Times in Photosynthetic Reaction Centers by Hole-Burning Spectroscopy. *J. Phys. Chem. Lett.* **2012**, *3*, 1684–1694.

(12) Novoderezhkin, V. I.; Romero, E.; Dekker, J. P.; van Grondelle, R. Multiple Charge-Separation Pathways in Photosystem II: Modeling of Transient Absorption Kinetics. *ChemPhysChem* **2011**, *12*, 681–688.

(13) Romero, E.; Augulis, R.; Novoderezhkin, V. I.; Ferretti, M.; Thieme, J.; Zigmantas, D.; van Grondelle, R. Quantum Coherence in Photosynthesis for Efficient Solar-Energy Conversion. *Nat. Phys.* **2014**, *10*, 676–682.

(14) Seibert, M. Biochemical, Biophysical, and Structural characterization of the Isolated Photosystem II Reaction Center Complex. In *The Photosynthetic Reaction Center, Vol. I*; Deisenhofer, J., Norris, J. R.; Eds; Academic: New York, 1993; pp 319–356.

(15) Tang, D.; Jankowiak, R.; Seibert, M.; Yocum, C. F.; Small, G. J. Excited-State Structure and Energy-Transfer Dynamics of Two Different Preparations of the Reaction Center of Photosystem II: A Hole-Burning Study. *J. Phys. Chem.* **1990**, *94*, 6519–6522.

(16) Tang, D.; Jankowiak, R.; Seibert, M.; Small, G. J. Effects of Detergent on the Excited State Structure and Relaxation Dynamics of the Photosystem II Reaction Center: A High Resolution Hole Burning Study. *Photosynth. Res.* **1991**, *27*, 19–29.

(17) Acharya, K.; Neupane, B.; Zazubovich, V.; Sayre, R. T.; Picorel, R.; Seibert, M.; Jankowiak, R. Site Energies of Active and Inactive Pheophytins in the Reaction Center of Photosystem II from *Chlamydomonas reinhardtii*. *J. Phys. Chem. B* **2012**, *116*, 3890–3899.

(18) Hillmann, B.; Brettel, J. K.; van Mieghem, F.; Kamlowski, A.; Rutherford, A. W.; Schlodder, E. Charge Recombination Reactions in Photosystem II. 2. Transient Absorbance Difference Spectra and Their Temperature Dependence. *Biochemistry* **1995**, *34*, 4814–4827.

(19) Nanba, O.; Satoh, K. Isolation of a Photosystem II Reaction Center Consisting of D-1 and D-2 Polypeptides and Cytochrome *b*-559. *Proc. Natl. Acad. Sci. U.S.A.* **1987**, *84*, 109–112.

(20) Seibert, M.; Picorel, R.; Rubin, A. B.; Connolly, J. S. Spectral, Photophysical, and Stability Properties of Isolated Photosystem II Reaction Center. *Plant Physiol.* **1988**, *87*, 303–306.

(21) Riley, K. J.; Zazubovich, V.; Jankowiak, R. Frequency-Domain Spectroscopic Study of the PS I–CP43' Supercomplex from the Cyanobacterium *Synechocystis* PCC 6803 Grown under Iron Stress Conditions. *J. Phys. Chem. B* **2006**, *110*, 22436–22446.

(22) Savikhin, S.; Xu, W.; Soukoulis, V.; Chitnis, P. R.; Struve, W. S. Ultrafast Primary Processes in Photosystem I of the Cyanobacterium *Synechocystis* sp. PCC 6803. *Biophys. J.* **1999**, *76*, 3278–3288.

(23) Jankowiak, R.; Tang, D.; Small, G. J.; Seibert, M. Transient and Persistent Hole Burning of the Reaction Center of Photosystem II. *J. Phys. Chem.* **1989**, *93*, 1649–1654.

(24) Krawczyk, S. The Effects of Hydrogen Bonding and Coordination Interaction in Visible Absorption and Vibrational Spectra of Chlorophyll. *Biochim. Biophys. Acta, Bioenerg.* **1989**, *976*, 140–149.

(25) Zucchelli, G.; Brogioli, D.; Casazza, A. P.; Garlaschi, F. M.; Jennings, R. C. Chlorophyll Ring Deformation Modulates Qy Electronic Energy in Chlorophyll-Protein Complexes and Generates Spectral Forms. *Biophys. J.* **2007**, *93*, 2240–2254.

(26) Chang, H.-C.; Jankowiak, R.; Reddy, N. R. S.; Yocum, C. F.; Picorel, R.; Seibert, M.; Small, G. J. On the Question of the Chlorophyll *a* Content of the Photosystem II Reaction Center. *J. Phys. Chem.* **1994**, *98*, 7725–7735.

(27) Jankowiak, R.; Rätsep, M.; Picorel, R.; Small, G. J. Excited States of the S-Chlorophyll Photosystem II Reaction Center. *J. Phys. Chem. B* **1999**, *103*, 9759–9769.

(28) Jankowiak, R.; Hayes, J. M.; Small, G. J. An Excitonic Pentamer Model for the Core Q_y States of the Isolated Photosystem II Reaction Center. *J. Phys. Chem. B* **2002**, *106*, 8803–8814.

(29) Diner, B. A.; Schlodder, E.; Nixon, P. J.; Coleman, W. J.; Rappaport, F.; Levergne, J.; Vermaas, W. F. J.; Chisholm, D. A. Site-Directed Mutations at D1-His198 and D2-His 197 of Photosystem II in *Synechocystis* PCC6803: Sites of Primary Charge Separation and Cation and Triplet Stabilization. *Biochemistry* **2001**, *40*, 9265–9281.

(30) Schlodder, E.; Renger, T.; Raszewski, G.; Coleman, W. J.; Nixon, P. J.; Cohen, R. O.; Diner, B. A. Site-Directed Mutations at D1-Thr179 of Photosystem II in *Synechocystis* sp. PCC 6803 Modify the Spectroscopic Properties of the Accessory Chlorophyll in the D1-branch of the Reaction Center. *Biochemistry* **2008**, *47*, 3143–3154.

(31) Romero, E.; van Stokkum, I. H. M.; Novoderezhkin, V. I.; Dekker, J. P.; van Grondelle, R. Two Different Charge Separation Pathways in Photosystem II. *Biochemistry* **2010**, *49*, 4300–4307.

(32) Romero, E.; Diner, B. A.; Nixon, P. J.; Coleman, W. J.; Dekker, J. P.; van Grondelle, R. Mixed Exciton–Charge-Transfer States in Photosystem II: Stark Spectroscopy on Site-Directed Mutants. *Biophys. J.* **2012**, *103*, 185–194.

(33) Krausz, E.; Hughes, J. L.; Smith, P.; Pace, R.; Peterson Årsköld, S. Oxygen-Evolving Photosystem II Core Complexes: A New Paradigm Based on the Spectral Identification of the Charge-Separating State, the Primary Acceptor and Assignment of Low-Temperature Fluorescence. *Photochem. Photobiol. Sci.* **2005**, *4*, 744–753.

(34) Shibata, Y.; Nishi, S.; Kawakami, K.; Shen, R.-J.; Renger, T. Photosystem II Does Not Possess a Simple Excitation Energy Funnel: Time-Resolved Fluorescence Spectroscopy Meets Theory. *J. Am. Chem. Soc.* **2013**, *135*, 6903–6914.